Reflectarray Antennas for 5-G Indoor Coverage

Álvaro F. Vaquero[1], Daniel R. Prado[2], Manuel Arrebola[1], Marcos R. Pino[1]
[1]Group of Signal Theory and Communications, Universidad de Oviedo, Spain, {fernandezvalvaro, arrebola, mpino}@uniovi.es
[2]Institute of Sensors, Signals and Systems, Heriot-Watt University, Edinburgh, U.K., dr38@hw.ac.uk

***Abstract*—A reflectarray antenna at 28 GHz is proposed to be used as a base station in 5-G indoor communications. The reflectarray is integrated in an office and the near-field radiated over a desktop surface is simulated. Since the near-field is not properly focused on the area defined for 5-G coverage, an optimization of the reflectarray is required. The generalized Intersection Approach algorithm is employed to optimize the radiated field at the plane of the desktop surface in order to improve the coverage area. Then, a comparison between the near-field before and after the optimization is carried out, showing a significant improvement of the coverage area. In addition, other planes are analyzed, allowing to extend the results from the optimized plane to others.**

***Index Terms*—Reflectarray, 5-G, indoor coverage, near-field, generalized Intesection Approach.**

I. INTRODUCTION

The rise of the 5G technology has sparked a need in the evolution of the communications systems to fulfill the new requirements. Currently, wireless communications work with high data rates and they must be faster and more sophisticated too. In addition, they must be ready to support a massive number of users and a wide range of applications including the fields of medicine, internet of things or drones. Consequently, the new generation is intended to work at higher frequency bands. In this way, millimeter-wave spectrum is considered as an excellent opportunity for the next 5G communications. Within the wide range of spectrum defined by the millimeter-wave, the greatest effort is focused on $28, 39$ and 60 GHz. In line with the development of this new generation, there are multiple goals that can be useful to improve many daily tasks such as achieving a total connectivity in a workstation. Nowadays, the work area in an office is full of devices that require connectivity, not only with external networks but also among them (laptop, tablets, mobile phones…). Due to this fact, instead of using base stations that radiate the power in many useless directions, it is more interesting to concentrate the whole power in a desired area, where all of these devices are placed. Thus, the use of near-field femtocells in indoor communications is a good solution to improve the operating efficiency of the base station and the comfort of the worker. In addition, the control of the near-field coverage area in this scenarios is more appropriate due to the complexity of the spot.

Regarding the base station antenna, it is necessary to shape the near-field in a desired area. On the other hand, the antenna should be compact, low-profile and embeddable with the environment since the antenna is placed into an office. Hence, a reflectarray is an ideal candidate to provide the coverage of a femtocell. The behavior of these antennas is virtually close to the parabolic reflectors. Thus, the reflectarray can be designed to collimate the field radiated by a feed in a given direction. There are several works which demonstrate the potential of these antennas in communications [1]. In [2] it was shown that it was possible to control the far-field, including the cross-polar component. Furthermore, in [3] the near-field of a reflectarray was optimized to be used in a CATR system. The fact that the near-field can be controlled is useful for its application to the design of specific near-field coverage areas. As reflectarrays antennas are suitable for manufacturing in microstrip technology, other advantages must be taken into account such as: lightweight designs and highly embeddable into indoor spots. Thus, in the next section an indoor setup is defined in order to analyze the behavior of a reflectarray antenna used as generator of a near-field coverage area. This includes the near-field coverage radiated by a reflectarray and how the coverage can be improved by applying an optimization of the antenna using the generalized Intersection Approach (IA) algorithm.

II. DESCRIPTION OF THE SCENARIO AND ANTENNA OPTICS

As it was mentioned before, in this work a reflectarray is proposed to be used as a base station of a femtocell in a work station. First, Fig. 1 shows a configuration of a conventional office, where the reflectarray is set parallel to the wall and the feed is placed at the ceiling. In this case, the feed illuminates the surface of the reflectarray, then the reflectarray collimates the field in the $\hat{z}_a$ direction, which depends on the angle θ_0. The coverage area is defined over the surface of the table. By doing so, all the devices within this area have connectivity. However, there are two main drawbacks in this configuration. First, the taper of the amplitude of the feed is reproduced in the reflected field as well as in the coverage area and its size can be very small. Apart from that, since the coverage area is not defined in a perpendicular plane to the $\hat{z}_a$ direction, the distribution of the copolar component of the electric field over the table will not have a proper shape for this purpose. In order to minimize the effect of both phenomena, an optimization applying the generalized IA is proposed in this work. Therefore, it is feasible to achieve a coverage area with a desired shape and required features.

Regarding the antenna, a planar reflectarray of 900 elements in a 30×30 regular grid has been chosen. The

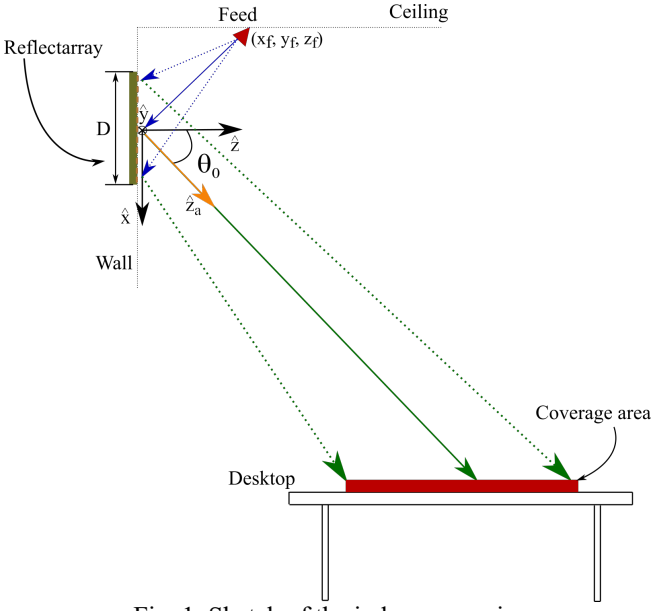

Fig. 1. Sketch of the indoor scenario.

periodicity in the $\hat{x}$ and $\hat{y}$ direction is 5×5 mm^2, thus the equivalent aperture is $D = D_x \times D_y = 150 \times 150$ mm^2 or $14\,\lambda \times 14\,\lambda$ at a central frequency of 28 GHz. Taking the center of the reflectarray as the center of the reference system, the feed is placed at $(x_a, y_a, z_a) = (-79.3, 0, 200)$ mm. In addition, the feed is modeled as an ideal horn with a $\cos^q \theta$ function and a q-factor of 20. The surface to be covered on the table is discretized in a uniform YZ grid at x-constant plane, $x = 1.62$ m. The limits of the grid are $y \in [-0.60, 0.60]$ m and $z \in [1.5, 2.5]$ m and the angle θ_0 is 30°.

III. NEAR-FIELD PHASE-ONLY SYNTHESIS

In this work, the phase-only synthesis technique used to shape the beam in the near-field region is based on the Intersection Approach (IA) algorithm. Unlike the classical optimization algorithms, the IA does not minimize a cost function but it seeks the intersection of two sets. If that is not possible, the IA finds out the minimum distance between both. The first set comprises the fields that fulfill the specifications (M). The other one is the set of the fields that can be radiated by the antenna (R), according to the antenna optics [4]. The projection of each set in the other is done by the definition of two projectors: the forward projector ($\mathcal{F}$) which projects the field from R onto M, and the backward projection ($\mathcal{B}$) that projects the field of the set M onto R. These projectors are used iteratively in the IA as follows:

$$\vec{E}_{i+1} = \mathcal{B}\left[\mathcal{F}(\vec{E}_i)\right] \tag{1}$$

where i is the current iteration and E the radiated field

Although in this work the synthesis is carried out only in magnitude, the algorithm allows the synthesis of both magnitude and phase. In order to apply the forward projection, it is necessary to define two templates with the upper and lower bounds for the whole volume where the near-field is computed. Once the computation is done, the field is trimmed applying the P_r^2 operator:

$$P_r^2(F) = \begin{cases} |T_{\max}(x,y)|^2, & |T_{\max}(x,y)| < |F(x,y)|^2 \\ |T_{\min}(x,y)|^2, & |F(x,y)|^2 < |T_{\min}(x,y)|^2 \\ |F(x,y)|^2, & \text{otherwise.} \end{cases} \tag{2}$$

where $T_{\max}(x,y)$ and $T_{\min}(x,y)$ are the templates of the upper and lower bounds respectively; $F(x,y)$ can be either the magnitude or the phase of the near-field.

Regarding the backward projection, there is a drawback when the optimization is in the near-field instead of the far-field. In the far-field case, the FFT is used as the backward projection [5], which is very efficient However, due to the impossibility of using this operator in the computation of the near-field, a new operator must be defined. Taking advantage of the distance definition in the Euclidean space L^2, the distance from an element belonging to the set M to the set R can be expressed as:

$$d = \iint_\Omega \left(|F'(x,y)|^2 - |F(x,y)|^2|\right)^2 dxdy \tag{3}$$

where $F'(x,y)$ can be either the magnitude or the phase of the near-field after applying the P_r^2 operator, obtaining a near-field that is within the boundaries; Ω is the surface of each plane where the near-field is computed.

Now, a general minimization algorithm such as the LMA [6] is able to minimize (3) and the minimum distance or the intersection between both sets may be found.

IV. RESULTS

A. Starting point

The starting point used in the synthesis process is the phase distribution corresponding to a reflectarray focused in the far field. In this case, the phase distribution can be computed as:

$$\phi_r(x_m, y_n) = \phi_{inc}(x_m, y_n) - k_0 x_i \sin\theta_0 \tag{4}$$

where $\phi_{inc}(x_m, y_n)$ is the incident field phase at the (m,n)-th element, k_0 is the vacuum wavenumber and θ_0 is the pointing direction, which in this case is $\theta_0 = 30°$ (see Fig. 1). This phase distribution is equivalent to the phase of the reflection coefficient for the X polarization (ρ_{xx}) and the optimization variables. Fig. 2 shows the phase distribution obtained for the setup described before.

This reflectarray focuses the field in a plane perpendicular to $\hat{z}_a$ direction. However, the coverage area is defined in a YZ cut. Thus, in this plane it does not focus the field. Instead, there are several maxima along $\hat{z}$ direction, see Fig. 3. In this figure, the red line represents the contour of the area to be covered, typically a table or a desktop. As shown in Fig. 3 and Fig. 4, there is a large amount of power that is radiated into a non-interest zone. Moreover, the surface of the table has a non-uniform distribution of the electric field.

The goal of the synthesis is to cover uniformly the zone, to maximize the power within the red lines and to minimize the power radiated in other directions.

B. Synthesis results

After 134 iterations of the algorithm, the optimization process converges and the resulting phase distribution is shown in Fig. 5. This phase distribution is close to the starting point, therefore it is smooth enough to be implemented in a proper prototype since the element design is straightforward using a zero-finding routine [7]. With regard to the obtained near-field, Fig. 6 shows the YZ cut and Fig. 7 shows the YZ and XZ cut. In the YZ cut, the different maxima along the $\hat{z}$ direction are concentrated into the boundaries of the coverage area. Hence, all the power that was radiated in non-interest directions before the optimization is now focused on the table, creating a unique coverage area. In addition, the field level in

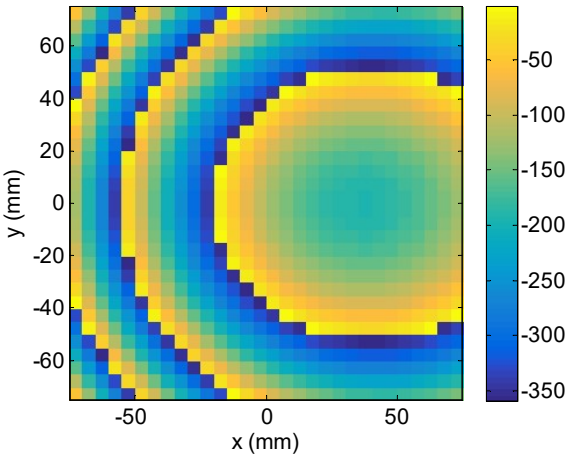

Fig. 2. Initial phase distribution for the copolar component in degrees.

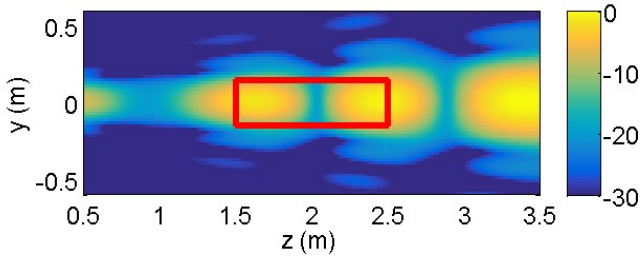

Fig. 3. Amplitude of the copolar component of the near-field normalized to the maximum in dB at $x = 1.62$ m. The red line shows the contour of the table or the coverage area.

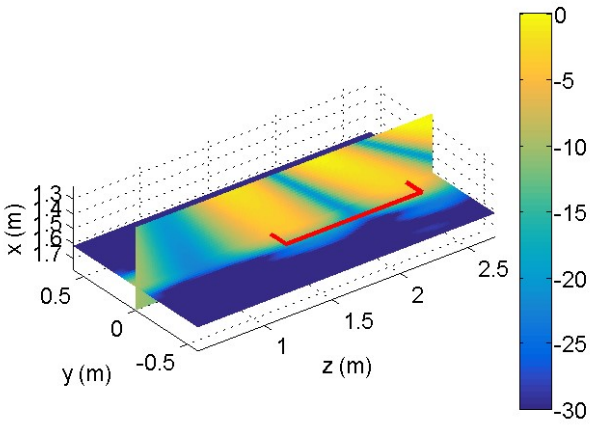

Fig. 4. Amplitude of the copolar component of the near-field normalized to the maximum in dB for the YZ and XZ cuts. The red line shows the contour of the table or the coverage area.

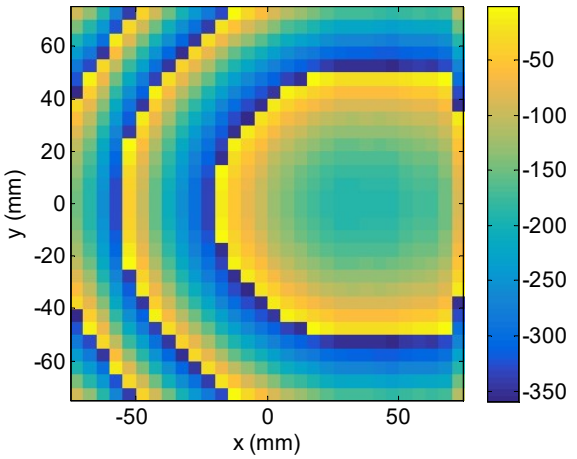

Fig. 5. Phase distribution of the reflectarray after the optimization process in degrees.

the surroundings of the table is at least -15 dB lower than the maximum.

Concerning to the XZ cut, the reflectarray successfully concentrates the power on the table surface after the optimization. However, there are still rays that disperse the power outside the considered plane as shown in Fig. 7. This happens since that region of space was not considered in the optimization. Therefore, a larger optimization grid with restrictions in the XY plane could improve the results presented in this work.

C. Depth of the coverage area

Since the synthesis is only carried out in one plane and not in a volume, it is interesting to study the radiated near-field at other planes. Therefore, the near-field is computed at the planes $x = 1.52$ m and $x = 1.72$ m. These results are shown in Fig. 8. Although the near-field is really close to the previous results in the plane $x = 1.62$ m, there are some differences

that must be taken into account. The shape of the near-field is similar in the three cases but in these two new planes the center is shifted either to the right or to the left, depending on the plane observed. Nevertheless, in light of these results, these two planes are similar to the central one and regarding that, those planes limit the depth of coverage area. Hence, although only one plane is optimized the results can be extended to the closest area.

V. CONCLUSION

An example of a reflectarray working as a base station for 5G indoor coverage is provided in this work. First, a setup where the reflectarray can be embedded and radiates the near-field over a desktop surface is defined. Then, the near-field over the desktop is analyzed. In light of the distribution of that near-field, an optimization using the generalized IA algorithm is carried out. The synthesis has been applied to the near-field amplitude by defining an upper and lower boundary templates. After the optimization process the coverage area is improved and the near-field is within specifications. In addition, the phase distribution is smooth, which increases the chance of achieving a successful design.

ACKNOWLEDGMENT

This work has been supported in part by the Ministerio de Ciencia, Innovación y Universidades under project TEC2017-86619-R (ARTEINE); by the Ministerio de Economía, Industria y Competitividad under project TEC2016-75103-C2-1-R (MYRADA); and by the Gobierno del Principado de Asturias under project GRUPIN-IDI-2018-000191 and through Programa "Clarín" de Ayudas Postdoctorales / Marie Courie-Cofund under project ACA17-09.

REFERENCES

[1] J.A. Encinar, M. Arrebola, G. Toso, "Design of a Tx/Rx Reflectarray Antenna for Space Applications" in *2th European Conference on Antennas and Propagation (EuCAP), Edinburgh, United Kingdom, Nov. 11-16, 2007,*

[2] D.R. Prado, M. Arrebola, M.R. Pino, F. Las-Heras, R. Florencio, R.R. Boix, J.A. Encinar, "Reflectarray antenna with reduced crosspolar radiation pattern" in *10h European Conference on Antennas and Propagation (EuCAP), Davos, Switzerland, Apr. 10-15, 2016,*

[3] A.F. Vaquero, D.R. Prado, M. Arrebola, M.R. Pino, F. Las-Heras, "Reflectarray probe optimization at millimeter frequencies" in *10h European Conference on Antennas and Propagation (EuCAP), Davos, Switzerland, Apr. 10-15, 2016,*

[4] O.M. Bucci, G.D'Elia, G. Mazzarella, and G. Panariello, "Antenna pattern synthesis: a new general approach", *Proc. IEEE*, vol. 82, no.3, pp. 358-371, Mar. 1994.

[5] J.A. Zornoza and J.A. Encinar, "Efficient phase-only synthesis of contoured-beam patterns for very large reflectarrays," *Int. J. RF Microw. Comput. Eng.*, vol. 14, no. 5, pp. 415-423, Sep. 2004.

[6] D.R. Prado, J. Álvarez, M. Arrebola, M.R. Pino, R.G. Ayestarán, and F. Las-Heras, "Effcient, accurate and scalable reflectarray phase-only synthesis based on the Levenberg-Marquardt algorithm," *Appl. Comp. Electro. Society (ACES) Journal,* vol. 30, no. 12, pp. 1246-1255, Dec. 2015.

[7] J. Huang and J.A. Encinar, *Reflectarray Antennas*. Hoboken, NJ, USA: John Wiley & Sons, 2008.

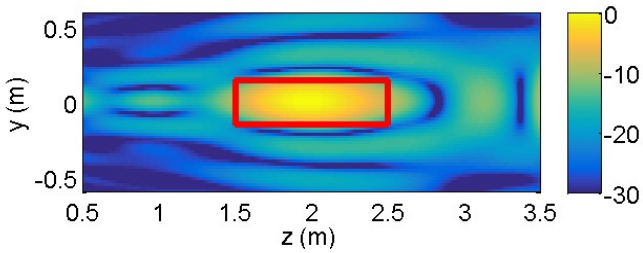

Fig. 6. Amplitude of the near-field normalized to the maximum in dB after the optimization. The red lines limit the area of the synthesis.

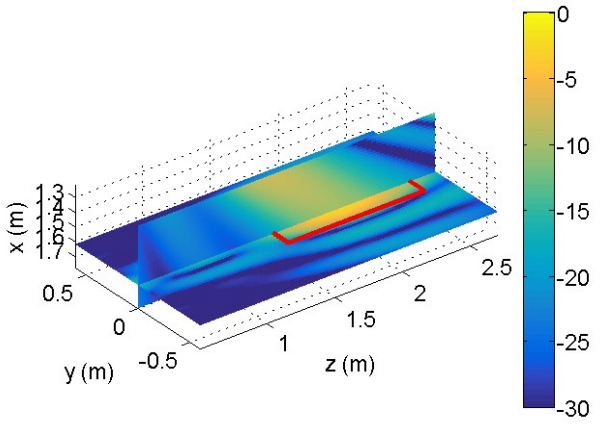

Fig. 7. Amplitude of the copolar component of the near-field normalized to the maximum in dB for the YZ and XZ cuts after the optimization. The red line shows the contour of the table or the coverage area.

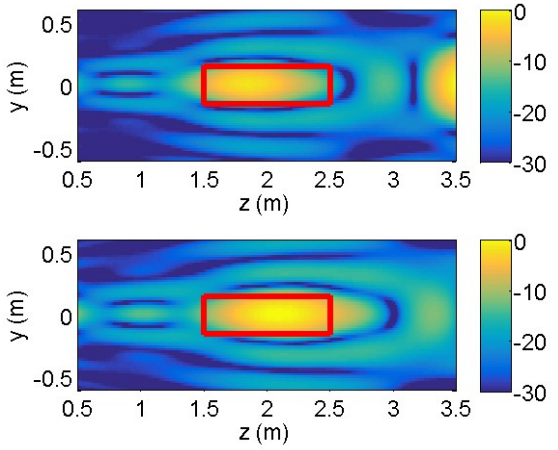

Fig. 8. Amplitude of the near-field after the optimization in $x = 1.52$ (top) and $x = 1.72$ (bottom) meters. The red lines limit the area of the synthesis.